DISK DISPERSAL AROUND YOUNG STARS

DAVID J. HOLLENBACH
NASA-Ames Research Center

HAROLD W. YORKE
Jet Propulsion Laboratory

and

DOUG JOHNSTONE
Canadian Institute for Theoretical Astrophysics

We review the evidence pertaining to the lifetimes of planet-forming disks and discuss possible disk dispersal mechanisms: (1) viscous accretion of material onto the central source, (2) close stellar encounters, (3) stellar winds, and (4) photoevaporation by ultraviolet radiation. We focus on (3) and (4) and describe the quasi-steady-state appearance and the overall evolution of disks under the influence of winds and radiation from the central star and of radiation from external OB stars. Viscous accretion likely dominates disk dispersal in the inner disk ($r \lesssim 10$ AU), whereas photoevaporation is the principal process of disk dispersal outside of $r \gtrsim 10$ AU. Disk dispersal timescales are compared and discussed in relation to theoretical estimates for planet formation timescales. Photoevaporation may explain the large differences in the hydrogen content of the giant planets in the solar system. The commonly held belief that our early sun's stellar wind dispersed the solar nebula is called into question.

I. INTRODUCTION

The question of planet formation is intimately related to the formation and evolution of disks around condensing protostars. When considering the evolution of dust grains through the planetesimal stage up to the creation of (proto)planets, it is important to realize that the disks themselves are continually evolving. Indeed, very short-lived disks may not have sufficient time to produce planets.

In the standard theory of low-mass star formation and disk evolution, a rotating, collapsing molecular core accretes at a rate $\dot{M}_c \sim 10^{-6}$–10^{-5} $M_\odot$ yr^{-1}, initially directly onto the protostar but soon mainly onto an orbiting accretion disk around the protostar (Terebey et al. 1984). This rapid accretion quickly builds up the disk mass M_d until gravitational instabilities set in, when the disk mass is roughly $\sim$0.3 $M_\star$, where $M_\star$ is the mass of

the protostar (Laughlin and Bodenheimer 1994; Yorke et al. 1995). The gravitational instabilities produce spiral density waves, which allow angular momentum to be transported outwards. The disk material can then be transferred onto the protostar at nearly the same rate as the disk accretes material from the molecular core; although this process may be quite episodic, the disk might roughly "hover" at the critical gravitationally unstable limit, $M_d \sim 0.3\ M_\star$, as the star grows. The result at the end of the accretion phase could be, for example, a 1-$M_\odot$ star with a $\sim$0.3-$M_\odot$ disk.

Once the cloud stops accreting onto the disk, the epoch of disk and stellar growth ceases. As the disk mass falls below the level required for gravitational instability, the transfer of angular momentum drops considerably, and other, less efficient processes for transport take over, possibly turbulent or magnetic (Balbus and Hawley 1991). This phase might be identified with the Class II, or T Tauri, phase of disk evolution, and observations of the excess blue emission from the accretion of the disk onto the star suggest median mass accretion rates of order 10^{-8} $M_\odot$ yr^{-1} with an order of magnitude scatter (Hartmann et al. 1998). As the disk loses mass, this rate should decrease. Whether the lifetime of the disk is thereafter determined by the evolution of the viscosity in the disk, which controls the accretion rate onto the star, or whether other processes such as winds and ultraviolet radiation eventually dominate disk dispersal, is part of the subject of this chapter.

Observational estimates of disk masses around young pre-main-sequence stars typically give values that are less than 10% the mass of the central star (Adams et al. 1990; Beckwith et al. 1990); often a value closer to 1% can be inferred. An example of an observationally well-determined and relatively high-mass disk is that of GM Aurigae (Koerner et al. 1993), a star of 0.72 $M_\odot$ with a disk of 0.09 $M_\odot$. In spite of some uncertainty in the mass estimates, these values for the later stages of disk evolution are in contrast to the theoretical values $\sim$0.3 $M_\star$ discussed above for disks still accreting material from the parent cloud. This might imply nonnegligible disk evolution after accretion stops.

The dust in the inner disks around low-mass stars apparently disappears in about 10^7 years, whereas disks around intermediate-mass stars appear to be depleted in somewhat shorter timescales (Strom 1995). Using pre-main-sequence evolutionary models to calculate the ages of star-forming clusters, and counting the numbers of stars found with and without observable inner disks, Strom showed that for very young ($\sim 10^6$ yr old) clusters such as Ophiuchus, almost all pre-main-sequence stars have disks, whereas for older regions the fraction of stars with disks drops as the stellar mass rises. A small fraction, perhaps 10%, of low-mass stars still have disks beyond 10 Myr. Therefore, the (inner) disk dispersal timescale for low-mass ($M_\star \lesssim 3$ $M_\odot$) stars may be of order $\tau_d \sim 10^7$ years.

These constraints on the evolution of the disk can be compared to models of the formation of giant planets in the solar system. Current theoretical thinking envisages a typical giant planet in the outer solar system to form by (1) the accumulation of solid (cometlike) planetesimals to ever larger bodies (Safronov 1969; Wetherill 1980; Nakagawa et al. 1983; timescale $\lesssim 10^5$ years, Weidenschilling 1984), until (2) a runaway growth occurs for the largest planetary embryos (Greenberg et al. 1978, 1984), with the runaway halted only after the depletion of the planetesimals in a given embryo's "feeding zone" and the embryos become gravitationally isolated from one another (at a mass $\sim 1\ M_\oplus$ in the giant planet region for a "minimum" solar nebula); followed by (3) a much slower agglomeration of individual embryos into the core of each of the current planets (Wetherill and Stewart 1986), until (4) the core reaches a critical mass (~ 15–$20\ M_\oplus$) and begins to gather in gas much faster than it gathers solids (Mizuno 1980; Bodenheimer and Pollack 1986; Pollack et al. 1996), followed yet later by (5) the cessation of gas and solid accretion, when tidal forces inside the Hill sphere suffice to open up a gap around the planet (Papaloizou and Lin 1984; Lin and Papaloizou 1985, 1986*a*,*b*). Protostellar disks can therefore be partially destroyed by the transformation of the gas and dust into planets.

However, it is clear that considerably more mass was dispersed by other mechanisms than was congealed into planets. If the solar nebula had only the "minimum mass" needed to form the known planets ($\sim 0.013\ M_\odot$ according to Hayashi et al. 1985), the timescale needed to assemble the giant planets ranges from $\sim 10^8$ yr for Jupiter to $\sim 10^{11}$ yr for Neptune (Nakagawa et al. 1983), much too long to explain many observed features of the solar system (such as the existence of the asteroid belt and of Neptune). Lissauer (1987, 1993) has proposed that the timescale problem can be alleviated by postulating a solar nebula that contained much more mass than the "minimum" value. Increases by a factor of 5–10 in the giant-planet zones would push the embryo isolation mass to or beyond the critical core mass, which would eliminate the slow process (3) of embryo accumulation, allowing Jupiter, Saturn, Uranus, and Neptune to form on timescales of $\sim 10^6$–10^8 yr. The core growth occurs then on timescales of $\sim 3 \times 10^6 (r/10\ \mathrm{AU})^{3/2}$ yr and the gas accretion onto the cores at times $\gtrsim 10^6$–10^7 yr.

Even if the solar nebula originated with only the minimum mass, there is clear evidence for disk dispersal by mechanisms other than planet formation. In accounting for the elemental abundances in the solar planets, one finds that the hydrogen and helium are deficient by a large factor compared to the original cosmic abundances that formed the planets. Clearly, the early solar nebula incorporated many of the heavier elements in the terrestrial planets and rocky cores, but substantial hydrogen- and helium-rich gas was dispersed by other mechanisms. Therefore, we conclude that planet formation is a minor disk dispersal mechanism. This chapter

focuses instead on the dispersal timescales of other mechanisms in order to understand the time available for the above processes of planet formation to operate.

A number of mechanisms, both internal and external, disperse the gas and dust disks around young stars or protostars. These processes can be so efficient that the disks may not have sufficient time to form planets, or the planets formed may be dispersed with the nebular material. For example, viscosity in the disk (see section II.A) coupled with the tidal force of a relatively massive disk on embedded giant planets may result in inwardly migrating planets that can be accreted, along with gas and dust, onto the central star (Lin et al. 1996). Close encounters with binary or cluster companions can strip and truncate the outer disks and can liberate the outer planets (section II.B). Stellar winds have often been postulated as a likely mechanism to entrain and push the gas and dust in the disk and to drive it into the interstellar medium (section II.C). The ultraviolet radiation from the central star or an external star can heat the outer disks and cause them to evaporate on relatively short timescales (section II.D). Obviously, understanding disk dispersal timescales is crucial to predicting the final products of planetary formation.

II. DISK DISPERSAL MECHANISMS

In our discussion of disk dispersal mechanisms, we shall focus on the dispersal of disk material at distances $\gtrsim 1$ AU from the central star, where terrestrial and giant planets may form and where the bulk of the mass of the young disk presumably resides, assuming a surface density distribution $\Sigma \propto r^{-\beta}$ with $\beta < 2$. We also focus on the early stages of disk evolution and the dispersal of the bulk of the original disk, rather than the later stages of dispersal of remnant disks, such as the one around β Pic. There are four basic processes for disk dispersal other than planet formation: (A) accretion of disk material onto the central source, (B) stripping due to close stellar encounters, (C) the removal of disk material due to the effects of stellar or disk winds, and (D) photoevaporation due to the ultraviolet radiation from the central source and/or close companions. All of these interactions operate concurrently, and we will discuss how winds can enhance photoevaporation. Considerable progress has been made since the last *Protostars and Planets* meeting in understanding the last of these mechanisms, so we devote a large proportion of our review to photoevaporation.

A. Disk Accretion

Radial mass flow in disks is a well-studied, although still not completely understood, phenomenon. The transport of angular momentum outward allows disk material to flow radially inward. The angular momentum can be transported, for example, by turbulence or magnetic fields, and often the physics of the evolution is subsumed in a parameter α that fixes the effective viscosity, which drives radial accretion through the disk.

Parameterizing the viscosity by $\nu = \alpha c_s H$ (Pringle and Rees 1972; Shakura and Sunyaev 1973), where scale height H and sound speed c_s are given by $H = r c_s/(GM_\star/r)^{1/2}$ and $c_s = (kT/m_H)^{1/2}$, we find $\nu \propto r$, if the temperature in the disk follows a $T \propto r^{-1/2}$ power law. Given that the viscous timescale $t_\nu \simeq r^2/\nu$, it follows that $t_\nu \propto r$:

$$t_\nu \simeq 10^5 \text{ yr} \left(\frac{\alpha}{0.01}\right)^{-1} \left(\frac{r}{10 \text{ AU}}\right)$$

The viscous dispersal timescale is plotted in Fig. 1 for two values of α (10^{-3} and 10^{-2}) thought to best represent the effective viscosity in protoplanetary disks (see, e.g., Hartmann et al. 1998). Assuming that disk angular momentum is constant and that the disk mass resides mostly at the outer disk radius r_d, it follows that $r_d(t) \propto M_d(t)^{-2}$. Therefore, as the disk accretes matter onto the central star, it preserves its angular momentum by expanding to greater size. For times greater than the initial timescale $t_{\nu 0}$,

$$r_d \simeq r_{d0}\left(\frac{t}{t_{\nu 0}}\right) \qquad \text{and} \qquad M_d(t) \simeq M_{d0}\left(\frac{t}{t_{\nu 0}}\right)^{-1/2}$$

where r_{d0} and M_{d0} are the initial radius and mass of the disk at $t_{\nu 0}$. As the disk grows, the viscous timescale in the outer regions, where the mass resides, gets longer. Therefore, viscous accretion may account for the

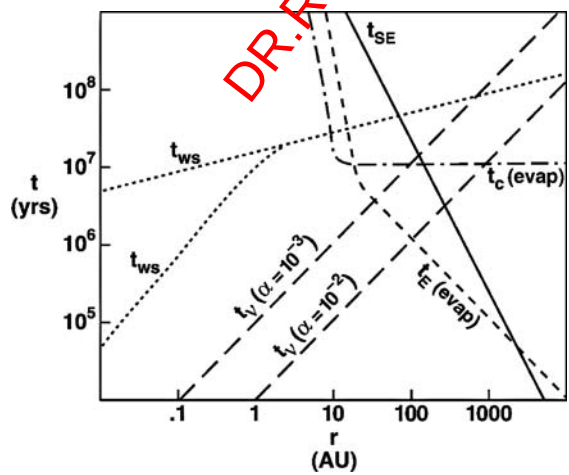

Figure 1. Timescales for disk dispersal: t_ν is the viscous timescale for $\alpha = 10^{-2}$ and 10^{-3}; t_{SE} is the stellar encounter (tidal stripping) timescale for Trapezium cluster conditions (see sections II.B and III); t_{ws} and t'_{ws} are stellar wind stripping timescales for wind and disk parameters summarized in section III; t_c (evap) is the photoevaporation timescale by the central star (strong wind case), and t_E (evap) is the photoevaporation timescale for an external star (Trapezium conditions) for the conditions summarized in sections II.D and III.

dispersal of the inner parts of disks, but it becomes insignificant for the outer disks and cannot explain the complete dispersal of the disk.

For $M_{d0} = 0.1\ M_\odot$ the mass accretion rate onto the central star, or the accretion mass loss rate from the disk, is given for $t > t_{\nu 0}$

$$\dot{M}_\nu \simeq 5 \times 10^{-7}\ M_\odot\ \mathrm{yr}^{-1} \left(\frac{\alpha}{0.01}\right)\left(\frac{r_{d0}}{10\ \mathrm{AU}}\right)^{-1}\left(\frac{t}{t_{\nu 0}}\right)^{-3/2}$$

B. Stellar Encounters

The effects of close stellar encounters on protostellar disks have been discussed by Clarke and Pringle (1993), Heller (1995), Hall et al. (1996), Larwood (1997), and Bonnell and Kroupa (1998). Typically, the disk (and any outer planets) is stripped to about $\frac{1}{3}$ the impact parameter r_p in a single close encounter. From this we can estimate the timescale t_{SE} to truncate a disk to the radius r_d: $t_{\mathrm{SE}} \simeq 1/n_\star \sigma v$, where $n_\star$ is the density of stars, $\sigma \simeq \pi(3r_d)^2$ is the collision cross section, and v is the velocity dispersion of stars:

$$t_{\mathrm{SE}} \simeq 2 \times 10^7\ \mathrm{yr} \left(\frac{n_\star}{10^4\ \mathrm{pc}^{-3}}\right)^{-1}\left(\frac{v}{1\ \mathrm{km\ s}^{-1}}\right)^{-1}\left(\frac{r_d}{100\ \mathrm{AU}}\right)^{-2}$$

This timescale is also shown in Fig. 1.

C. Effects of Winds on Disks

Although protostellar winds and outflows were a great surprise when first observed some two decades ago, we are now beginning to understand the origin of the winds and the wind environment in the vicinity of circumstellar disks. During and after the cloud collapse phase, which builds up the disk mass, the disk actively accretes onto the protostar ($t \lesssim 10^7$ yr) and creates a strong wind. The interaction of the rotating magnetic field with the inner disk produces this wind, whose mass loss rate ($\dot{M}_w \sim 10^{-7}\ M_\odot\ \mathrm{yr}^{-1}$ [for $t \sim 10^6$ yr] to $10^{-8}\ M_\odot\ \mathrm{yr}^{-1}$ [for $t \sim 10^7$ yr]) is about 0.3–0.5 times the accretion rate onto the protostar (Shu et al. 1988; Königl 1995; Ouyed and Pudritz 1997*a*,*b*). The terminal wind speeds are of order 100–200 km s^{-1}. The mass lost in these strong winds is disk material ejected via coupling between the (weakly) ionized disk gas and the outward-bending magnetic field. These disk winds are not spherically symmetric but are magnetically collimated away from the disk plane toward the poles. Later, as the accretion subsides, the magnetic activity in the chromosphere of the young, low-mass star drives a (spherically symmetric) stellar wind, which is likely much more active in the early ($\sim 10^7$ yr) epoch than the current solar wind ($\dot{M}_w \sim 10^{-14}\ M_\odot\ \mathrm{yr}^{-1}$).

As an upper limit to the dispersing power of disk winds, we will ignore their collimation and consider the momentum transferred by the collision of spherically symmetric winds with the disk (Fig. 2). The scale height of cold [$c_s \sim 0.1\,(GM_\star/r)^{1/2}$] protostellar disks is of order $H \sim 0.1r$, which

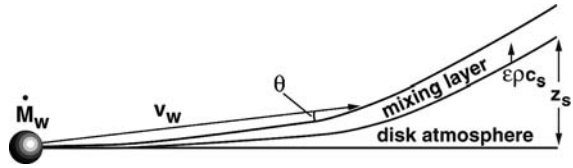

Figure 2. Schematic representations of the stripping of disk material due to the shear caused by the impact of a stellar wind.

implies that the fraction of solid angle subtended by cold disks is of order 0.1. Assuming that stripping occurs in a thin mixing layer at a height $z_s(r)$ above the disk and that disk gas flows into this mixing region at a velocity of ϵc_s, where ϵ must be less than unity and has been estimated to be $\simeq$0.01–0.1 by Canto and Raga (1991), the mass loss rate can be approximated by $\dot{M}_{\rm ws} = 2\int_{r_\star}^{r_d} \epsilon\rho(r, z_s)\, c_s(r)\, 2\pi r\, dr$. In the thin mixing layer at $z_s(r)$, the normal component of the wind ram pressure $(\sin\theta)^2\,(\dot{M}_w v_w/4\pi r^2)$ equals the disk gas pressure $\rho(r, z_s)\, c_s^2(r)$, where θ is the angle between the incident wind and the wind shock, which traces the top of the mixing layer. Substituting this relation into the mass loss equation and assuming that $c_s(r)$ declines with r, we conclude that the maximum mass loss rate $\dot{M}_{\rm ws}$ and the minimum dispersal timescale $t_{\rm ws}$ from wind stripping are given by

$$\dot{M}_{\rm ws} \simeq 4\times 10^{-2}\,\dot{M}_w \left(\frac{v_w}{100\ {\rm km\ s^{-1}}}\right)\left(\frac{\epsilon\overline{(\sin\theta)^2}}{10^{-4}}\right)\left(\frac{T(r_d)}{100\ {\rm K}}\right)^{-1/2}$$

and

$$t_{\rm ws} \simeq 10^7\ {\rm yr}\left(\frac{r}{1\ {\rm AU}}\right)^{1/4}\left(\frac{\epsilon\,(\sin\theta)^2}{10^{-4}}\right)^{-1}\left(\frac{M_d}{M_{\rm min}}\right) v_{w7}^{-1}\dot{M}_{w-8}^{-1}$$

where $v_{w7} = v_w/100\ {\rm km\ s^{-1}}$, $\dot{M}_{w-8} = \dot{M}_w/10^{-8}\ {\rm M_\odot\ yr^{-1}}$, $\overline{(\sin\theta)^2}$ is the integral-averaged value of $(\sin\theta)^2$, and $M_{\rm min} \simeq 0.01\ {\rm M_\odot}$ is the minimum mass solar nebula. We have numerically computed $\overline{(\sin\theta)^2} \sim 10^{-3}$ for a reference model with $\dot{M}_{w-8} = 1$, $v_{w7} = 1$, and $M_d = M_{\rm min}$.

Stellar wind dispersal has been postulated as a mechanism for the dispersal of stellar disks (Cameron 1973; Horedt 1978, 1982; Elmegreen 1979). However, as can be seen in Fig. 1, where various disk dispersal timescales are compared to one another, wind stripping should not be an effective disk dispersal mechanism for a reasonably flat (cold) disk, assuming $\epsilon(\sin\theta)^2 \lesssim 10^{-4}$.

Three separate arguments support this conclusion. First, Richling and Yorke (1997) have done numerical simulations that include the ultraviolet-induced photoevaporation of the disk (see section II.D below) acting simultaneously with (isotropic) wind stripping. The ultraviolet-heated disk

atmosphere and photoevaporative flow deflect and collimate the wind and reduce the wind stripping significantly. A low degree of mixing between the winds and the disk outflows is found. Although no numerical simulations exist for the particular configuration of interacting T Tauri disks and winds, one can infer from the results of Richling and Yorke (for disks around high-mass stars) that the value for $\epsilon(\sin\theta)^2$ is indeed low. Secondly, we note that the strong protostellar (disk) winds collimate quickly, probably by magnetic forces, and for this reason alone are unlikely to aid in the removal of material from the outer disk; see, for example, recent Hubble Space Telescope (HST) images of DG Tau (Kepner et al. 1993) and HH30 (Stapelfeldt et al. 1994; Burrows et al. 1996). Finally, if the powerful winds around young stars are powered by disk accretion, it is unlikely that they can remove the entire disk.

Further work should be done to test for instabilities that could significantly raise ϵ and to study the parameter space of disk properties exhaustively to test the variations in $(\sin\theta)^2$. In the absence of these results, the wind dispersal timescales plotted on Fig. 1 [$t_{\rm ws} \equiv \Sigma(r)/\dot{\Sigma}(r)$, where $\Sigma(r)$ is the surface density at r] are only improved versions of previous work, still uncertain by perhaps an order of magnitude. Nevertheless, we suggest that wind stripping is probably not as significant as viscous accretion and photoevaporation.

D. Photoevaporation

Disk photoevaporation was first proposed for high-mass stars with disks, because these stars have extremely powerful Lyman continuum fluxes. One of the main motivations was to explain the relatively long lifetimes of small ($r \lesssim 10^{17}$ cm) and dense ($n_e \gtrsim 10^4$–10^5 cm^{-3}) ultracompact H II (UC H II) regions. The high densities and temperatures of these regions compared to molecular clouds as a whole suggest that UC H II regions are overpressurized and should expand at velocities in excess of $c_s \sim 10$ km s^{-1}. Without replenishment of this gas, the dynamical timescale of $\sim 10^{3.5}$ yr predicts that these regions should quickly expand and become more diffuse. However, Wood and Churchwell (1989) performed a radio survey of UC H II regions and found that 10–20% of all O stars are in the UC H II phase. Given that O stars live approximately 10^{6-7} yr, this implies that dense UC H II regions last for $10^{5.5}$ yr, two orders of magnitude longer than the dynamical timescale.

Whereas the idea of using the photoevaporation process as a means for eroding disks around young massive stars had been mentioned occasionally in the literature (e.g., Bally and Scoville 1982), Hollenbach et al. (1993, 1994) first applied the idea rigorously as a model for ultracompact H II regions. The first numerical studies of this process (Yorke and Welz 1993, 1994) have been supplemented by more realistic simulations including the effects of UV dust scattering (Richling and Yorke 1997) and photoevaporating the disks of close companions in a multiple system

(Richling and Yorke 1998, 1999). Hollenbach et al. (1994) proposed that UC H II regions live for $10^{5.5}$ yr because they are constantly being replenished by a dense circumstellar reservoir: the orbiting disk. Although the high-pressure gas expands away from the disk at speeds of 10–50 km s^{-1}, the disk reservoir maintains a quasi-steady-state density and intensity profile. The photoevaporating disk model matches well with the morphology, emission measure, and spectrum of numerous UC H II regions. As we shall demonstrate below in section II.D.1, the mass loss rate $\dot{M}_{\rm ph}$ from the disk around an O star with a Lyman continuum photon luminosity $\Phi_i \sim 10^{49}$ s^{-1} is of order a few times 10^{-5} $M_\odot$ yr^{-1}. Therefore, if massive O stars are born with disks with mass ~0.1–0.3 $M_\odot$, the timescale to photoevaporate the disk is $10^{5.5}$ years. Although this timescale is long enough to explain UC H II regions, it is sufficiently short to have significant impact on the formation of planets around high-mass stars.

Surface disk material evaporates efficiently when it is heated to temperatures such that the average thermal speeds of the atoms or ions are comparable to the escape speed from the gravitational potential. Photoionization of hydrogen by Lyman continuum (extreme ultraviolet or EUV, $h\nu > 13.6$ eV) photons heats the gas at the surface of the disk to temperatures $T \sim 10^4$ K, forming an ionized atmosphere or corona above the disk. Beyond a critical distance from the central star, $r_g \simeq GM_\star/c_s^2$ ($\sim 10^{14}\,[M_\star/M_\odot]$ cm), the heated gas becomes unbound and produces a thermal disk wind. Massive stars radiate copious EUV photons, which rapidly photoevaporate their outer disks. Young low-mass stars also have sufficient Lyman continuum flux to photoionize their outer disk material and create an appreciable photoevaporative flow. Alternatively, nearby massive stars in star-forming regions produce large fluxes of both EUV and FUV (for ultraviolet, 6 eV $< h\nu <$ 13.6 eV) photons, which can heat and evaporate the circumstellar disks around young low-mass stars.

1. Photoevaporation by the Central Star: Physical Processes and Semianalytical Models. The ultraviolet flux from the central star can be divided into the EUV, capable of ionizing hydrogen, and FUV, capable of dissociating H_2 and CO and ionizing C. The EUV flux ionizes and heats the surface of the disk to 10^4 K. The FUV flux penetrates the H II region created by the EUV flux and heats a primarily neutral layer of H and H_2 to temperatures of order 100–3000 K, depending on the magnitude of the flux and the density of the gas. These regions in the interstellar medium are often called photodissociation regions, or PDRs (e.g., Hollenbach and Tielens 1997).

Previous work has treated the effect of EUV photons, and we shall focus on that case here. However, the FUV photoevaporation by the central star is nearly completely analogous, and we will remark on the small differences for this case as they arise. We will also normalize our equations for the case of the photoevaporation by a low-mass ($M_\star = 1\,M_\odot$) star, with an estimated EUV photon luminosity of 10^{41} s^{-1}. However, the equations

are equally applicable to high-mass stars (indeed, as noted above, they were originally derived for this case).

Weak stellar wind case. If the central star has a "weak" stellar wind (we shall quantitatively describe the criterion for a weak wind below), then photoionization of the neutral hydrogen on the surface of the inner region of the disk should result in the formation of a bound ionized atmosphere with $T \sim 10^4$ K (c.f. Fig. 3a). Inside $r_g \simeq 10$ AU $M_\star/\mathrm{M}_\odot$, where the sound velocity is less than the escape velocity, the atmosphere can be approximated as hydrostatic and isothermal. The density of ionized hydrogen $n(r,z)$ in the inner region depends on the density at the base of the H II atmosphere $n_0(r)$ and the height z above the disk according to $n(r,z) = n_0(r)\exp(-z^2/H^2)$, where the scale height is given by: $H(r) = r^{3/2}/r_g^{1/2}$ (Hollenbach et al. 1994). Note that $H(r_g) = r_g$.

Outside of r_g the evaporated material flows from the disk at approximately the sound speed $v \sim c_s \simeq 10$ km s^{-1}. Here, $n(r,z) \simeq n_0(r)$ yields a reliable estimate near the disk ($z < r$), where the flow has little opportunity to expand. The mass loss rate from the disk $\dot{M}_{\rm ph}$ is given by $\dot{M}_{\rm ph} = 2m_{\rm H}c_s \int_{r_g}^{\infty} 2\pi n_0(r) r\, dr$, where the first factor of 2 accounts for both faces of the disk and $m_{\rm H}$ is the mass per hydrogen nucleus. A similar re-

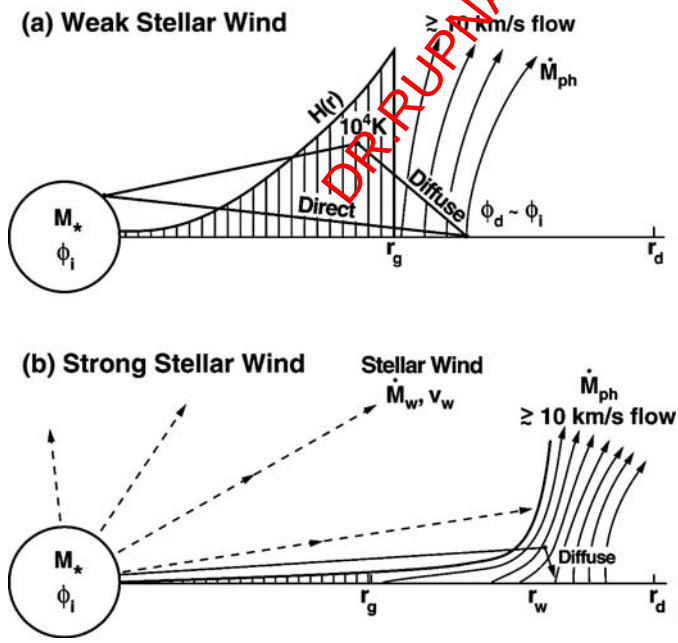

Figure 3. Schematic representation of photoevaporation by the central star. On the top (a) is the case with insignificant stellar wind. On the bottom (b) is the strong wind case. The scale height $H(r)$ of the disk is shown in (a), along with typical paths of direct and diffuse EUV photons.

lationship holds for flows controlled by FUV, where the sound speed is of order 1 to 3 km s^{-1} and r_g is correspondingly increased.

Estimating the mass loss rate and dispersal timescale of a disk by photoevaporation therefore reduces to determining $n_0(r)$, constrained by the above equations for $n(r, z)$ and $H(r)$, such that the UV photons are just absorbed at the base of the H II atmosphere or flow. For EUV photons, the recombination of electrons and protons in the ionized H II surface layers leads temporarily to H atoms, which absorb EUV photons and become reionized. Therefore, both dust and recombinations provide a source of opacity, which attenuates the incident EUV flux. A self-regulating feedback mechanism is established. The base density $n_0(r)$ adjusts itself so that EUV photons are nearly completely absorbed by the time they reach the base (i.e., there is an ionization front at the base). If $n_0(r)$ were lower than this value, the EUV photons would penetrate deeper into the dense neutral disk and would reach a higher $n_0(r)$. On the other hand, if the density were higher than this value, then the recombinations or dust in the overlying gas would provide such high opacity that the EUV photons would not penetrate to the base, which is contradictory.

In the case of EUV photons, both the recombinations in the atmosphere and flow as well as the scattering from dust in these regions provide a source of *diffuse* EUV photons. Approximately one-third of the recombinations is to the ground state of H, which produces isotropically radiated EUV photons. Hollenbach et al. (1994) show that the atmosphere absorbs a significant fraction of the EUV photon luminosity, Φ_i, of the central star and that the diffuse field dominates the direct EUV flux from the star in determining $n_0(r)$. In the case of FUV photons, dust scattering alone provides a diffuse source of photons, but this case has not yet been quantitatively analyzed. The dust grains that dominate the scattering and absorption at EUV and FUV wavelengths have typical radii $\sim$100 Å. These small dust particles tend to remain in the upper atmospheres of the disks for substantial periods before settling and coagulating (Weidenschilling 1984, see also section II.D.4). However, if they do clump together and rain out from the upper layers of the disk in the absence of turbulence (e.g., Cameron 1995), the scattering could be reduced significantly.

Hollenbach et al. (1994) find an analytic solution for the case of EUV photons in the bound ($r < r_g$) region. They find that $n_0 \propto r^{-3/2}$ in the static region, whereas beyond the static region the power law steepens to $n(r) \propto r^{-\gamma}$, where $\gamma \gtrsim \frac{5}{2}$. Most of the mass loss occurs, then, in the region just outside of r_g. A complete analysis finds

$$\dot{M}_{\rm ph} = 4 \times 10^{-10}\ {\rm M}_\odot\ {\rm yr}^{-1} \left(\frac{\Phi_i}{10^{41}\ {\rm s}^{-1}}\right)^{1/2} \left(\frac{M_\star}{{\rm M}_\odot}\right)^{1/2}$$

where $\Phi_i \sim 10^{41}\ {\rm s}^{-1}$ is a crude estimate of the EUV luminosity of a young (less than 10^7 yr old) solar-type star (see section II.D.3 below). Both within and beyond the static region the ionized hydrogen is maintained primarily

from diffuse photons produced in the atmosphere. The dominance of the diffuse field means that the exact shape of the thin disk does not enter (shadowing is not important). In addition, the radiative transfer ensures that $n_0(r)$ and $\dot{M}_{\rm ph}$ do not depend on the surface density distribution of the disk, as long as it is sufficient to maintain a dense neutral disk under the H II surface.

Numerical simulations of disks photoionized by a central EUV source with a weak stellar wind have been performed by Yorke and Welz (1994, 1996) and by Richling and Yorke (1997). Richling and Yorke (1997) include the effects of dust scattering and find a similar power law dependence of $\dot{M}_{\rm ph}$ on Φ_i (exponent ≈ 0.58) and comparable mass loss rates for high-mass stars ($\Phi_i \sim 10^{49}$ s^{-1}) in the range $10^{-7} \lesssim \dot{M}_{\rm ph}/\,{\rm M}_\odot\ {\rm yr}^{-1} \lesssim 10^{-5.5}$. However, the numerical simulations employed finite disks with central holes, whereas the disks discussed here are considered to extend from the stellar surface until $r \gg r_g$.

Strong stellar wind case. In the case of a strong wind from the central star, the ram pressure of the stellar wind, $\rho_w v_w^2$, will be too high for a static atmosphere to achieve a full scale height above the disk. Instead, the stellar wind will suppress the height of the ionized layer out to a radius $r_w > r_g$, where the thermal pressure of the ionized hydrogen flowing from the disk balances $\rho_w v_w^2$ (see Fig. 3b). The photoevaporated material can freely flow vertically off the disk at radii beyond $r_w \simeq 10$ AU $\dot{M}_{w-10}^2 v_{w7}^2 \Phi_{41}^{-1}$, where $\dot{M}_{w-10} = \dot{M}_w/10^{-10}$ M$_\odot$ yr^{-1}, $v_{w7} = v_w/100$ km s^{-1}, and $\Phi_{41} = \Phi_i/10^{41}$ s^{-1}. The criterion for a strong wind, $r_w > r_g$, can be written that the stellar wind mass loss rate $\dot{M}_w$ exceeds a critical value $\dot{M}_{\rm cr} = 4 \times 10^{-11} \Phi_{41}^{1/2} M_0^{1/2} v_{w7}^{-1}$ M$_\odot$ yr^{-1}, where $M_0 = M_\star/\,{\rm M}_\odot$ (Hollenbach et al. 1994). Although there are large uncertainties in both $\dot{M}_w$ and Φ_i for young low-mass stars, it appears that the strong wind condition may often be met. With fewer uncertainties, it also is generally met for O and B stars (van Buren 1985).

The overall effect of the stellar wind is to allow EUV flux to penetrate more readily to the disk surface in the flow ($r > r_g$) region, which enhances the photoevaporative mass loss rate. Hollenbach et al. (1994) find, for the strong wind conditions, $\dot{M}_w > \dot{M}_{\rm cr}$,

$$\dot{M}_{\rm ph} \simeq 4 \times 10^{-10}\ {\rm M}_\odot\ {\rm yr}^{-1} \left(\frac{\dot{M}_w}{10^{-10}\ {\rm M}_\odot\ {\rm yr}^{-1}}\right)\left(\frac{v_w}{100\ {\rm km\ s}^{-1}}\right)$$

The photoevaporative mass loss rate from the outer disk now becomes slightly more than the mass loss rate in the assumed isotropic stellar wind. We emphasize that these approximate analytical solutions hold only when the disk extends to $r_d > r_w$.

The photoevaporation timescale t_c(evap) caused by the central star in a strong wind case is also plotted in Fig. 1. Here we have assumed that $r_w > r_d$, so $n_0 \propto r^{-3/2}$ from r_g to r_d (Hollenbach et al. 1994), and that $\beta = 3/2$, $\Phi_i = 10^{41}$ s^{-1}, and a minimum mass nebula. Since $\Sigma \propto r^{-3/2}$

is assumed, the photoevaporative timescale becomes independent of r for $r > r_g$:

$$t_c(\text{evap}) \simeq 10^7 \text{ yr} \left(\frac{\Phi_i}{10^{41} \text{ s}^{-1}}\right)^{-1/2} \left(\frac{\Sigma_0}{\Sigma_0(\text{min})}\right)$$

where Σ_0 is the disk surface density at a fiducial radius and Σ_0(min) is the corresponding value for the minimum solar nebula.

A strong wind also affects the radiative transfer in two important ways. First, if it is partially neutral, it is a source of opacity for the EUV photons trying to travel from the star to r_g. Therefore, it could significantly lower the ratio of EUV to FUV photons arriving at r_g from the star. Secondly, the ionized material in the wind will recombine and thereby produce a "diffuse" source of EUV and FUV photons above the disk. Many of the EUV photons will be absorbed "on the spot" by the neutral component of the wind. These effects should be addressed quantitatively in the future.

Although no analytic solution has been proposed for a central star that radiates only FUV photons, the outline of the solution is clear. Whereas both hydrogen atoms and dust are opacity and scattering sources for EUV photons, dust alone dominates the FUV opacity. Dust also scatters the FUV (the albedo of interstellar dust is typically ~0.3–0.6 in the FUV), and the isotropic component of the scattering produces a diffuse FUV field. The critical gravitational radius is now further out, because $r_g \propto c_s^{-2}$ and the PDR surface gas is cooler than 10^4 K. Again, the EUV and FUV flux from the wind should be evaluated.

The above analytic solutions (Hollenbach et al. 1994) made simple analytic approximations for the dynamics of an evaporating disk (e.g., $v_z = 0$ for $r < r_g$ and $v_z = c_s$ for $r > r_g$) and for the radiative transfer solution for the diffuse EUV field. In order to consider various effects such as disk evolution, non-steady-state heating/cooling, and ionization/recombination, as well as more detailed hydrodynamic interactions and radiative transfer, numerical simulations are required.

2. Photoevaporation by the Central Star: Numerical Simulations. The first numerical simulations of the evolution of circumstellar disks subjected to the influence of EUV photons from the central source were discussed by Yorke and Welz (1993) as a model for UC H II regions. Although the effects of disk rotation, self-gravity, IR heating of the dust, time-dependent heating and cooling, and hydrogen ionization and recombination were included in the 2D axially symmetric hydrodynamic code, these early models considered the direct stellar EUV flux only; sharp shadows were cast by the disk. Including the effects of the diffuse EUV field produced by recombinations directly into the ground state (Yorke and Welz 1994, 1996) allowed the ionization front to wrap around and envelop the disk, but these "soft" EUV photons were able to heat the ionized material in the disk's shadow regions only to ≈2000 K, much lower

than the value ≈8000 K of the ionized material directly illuminated by the central star. Richling and Yorke (1997) found that if the effects of UV dust scattering were included, the "shadow" regions quickly disappeared and the ionized gas attained temperatures ≈8000 K everywhere. The mass loss rate was enhanced by a factor of about 2 for UV dust opacities $\kappa_{uv} = 200\ \mathrm{cm^2\ g^{-1}}$. The top two panels of Fig. 4 show results from their numerical simulations of stars with no stellar winds. This scattering result is for the case of high-mass stars, which produce relatively high (∼1) dust optical depths in the disk atmosphere. Solar type stars will produce much lower dust optical depths, and will show much less effect from dust scattering.

For the cases with strong stellar winds, Yorke and Welz (1996) and Richling and Yorke (1997) find a much weaker dependence of the disk mass loss rate with wind velocity (a power law exponent 0.1 rather than 1) when compared to the analytic models discussed here and by Hollenbach et al. (1994). Because, however, the numerical simulations consider cases of very massive disks $M_d \gtrsim 0.2\ M_\star$ with a central cavity and a finite outer radius r_d of order r_w, they are not readily comparable to the analytic results, which assume $r_d \gg r_w$ and no central cavity. In the numerical simulations the originally isotropic stellar wind interacts with the outflowing photoevaporation flow from the disk to produce shocks in both the wind material and the photoevaporation flow, which are separated by a contact discontinuity (see bottom panel of Fig. 4, from Kessel et al. 1998). The shock-heated wind material seeks the easiest path of escape, which is along the rotational axis. A hydrodynamically collimated bipolar outflow results, the opening angle of which increases slowly with increasing wind velocity. For warm ($T \approx 10^4$ K), low-velocity ($v_w \approx 50\ \mathrm{km\ s^{-1}}$) winds, the mass loss rate due to photoevaporation $\dot{M}_{ph}$ actually *decreases* with increasing stellar wind mass loss $\dot{M}_w$, because the wind itself absorbs EUV photons.

3. Photoevaporation of the Solar Nebula by the Sun and the Formation of the Giant Planets. The introduction to this chapter presents the current picture of giant planet formation and concludes that (1) this process is a minor disk dispersal mechanism and (2) $M_d \approx$ several M_{min}. As discussed by Shu et al. (1993), several serious issues remain in this picture. What dispersed all the residual gas in this enhanced-mass nebula? Removing ∼0.1 $M_\odot$ of gas stored in a thin disk by a T Tauri wind (mass loss rate $\sim 10^{-8}\ M_\odot\ \mathrm{yr^{-1}}$ for 10^7 yr) is a questionable proposition, whereas transporting this much material inward to the center by viscous accretion would push any planet (like Jupiter) that has cleared a gap around itself also into the sun (for the basic dynamical mechanisms, see Goldreich and Tremaine 1979, 1980; Lin and Papaloizou 1979, 1985; Hourigan and Ward 1984; Ward 1986).

Even if we ignore the timescale problem for accumulating critical cores for the giant planets and assume that the giant planets somehow formed under conditions that resembled the minimum solar nebula, we

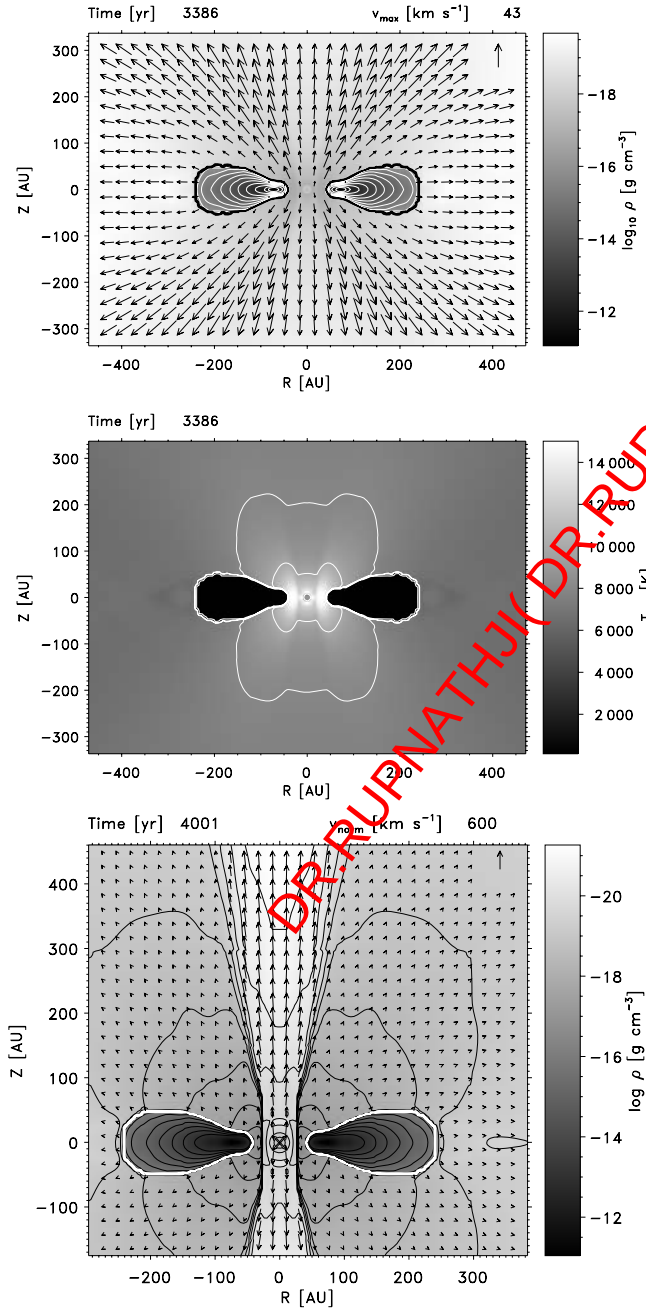

Figure 4. Numerical simulations of the photoionization and photoevaporation of circumstellar disks by a central EUV source (Richling and Yorke 1997). Top: Density (gray scale + contours), ionization front (thick line) and velocity structure (defined at tips of arrows; the velocity scale is given at the upper right of each frame) are shown long after a quasi-steady-state flow has been achieved. Middle: The corresponding temperature structure is displayed. Bottom: The resulting quasi-steady-state structure of a simulation that included the effects of a central stellar wind (Kessel et al. 1998).

run into a second difficulty: the delicate timing between core growth and nebula dispersal that must seemingly be achieved to yield the differential results that we observe for the masses of the gaseous envelopes of the four giant planets. The rock-ice cores of the giant planets are all about 15 Earth masses ($M_\oplus$), but the hydrogen/helium envelopes for Jupiter, Saturn, Uranus, and Neptune contain ~300, ~75, ~2, and ~2 $M_\oplus$ respectively (Shu et al. 1993). Note that there is a sharp cutoff in hydrogen/helium mass between Saturn and Uranus, even though the core masses are similar and are presumably large enough in Uranus and Neptune to initiate the rapid accumulation of hydrogen and helium gas. The problem arises because most theories of disk dispersal by thermal evaporation or solar wind erosion (e.g., Cameron 1978; Elmegreen 1978; Horedt 1978, 1980, 1982; Sekiya et al. 1980; Pechernikova and Vitjazev 1981; Ohtsuki and Nakagawa 1988) predict gas loss rates that vary smoothly with time and radial position in the disk, whereas the usual core instability picture demonstrates that the process of runaway gas gathering proceeds very quickly once it gets going. Adjusting the parameters appropriately to explain Jupiter and Neptune will typically leave Uranus and Saturn complete mysteries. The problem then becomes to identify the gas removal mechanism that would satisfactorily explain the sharp differences in envelope masses between the gas-rich giants, Jupiter and Saturn, and the gas-poor giants, Uranus and Neptune.

Shu et al. (1993) point out an interesting coincidence between $r_g \approx 10$ AU for the solar system and the radial position that separates the gas-rich giants from the gas-poor ones. The transition between photoionized gas being gravitationally trapped in the solar nebula and flowing off in an evaporative wind occurs roughly at the orbital distance of Saturn. If the photoevaporative rate of mass loss $\dot{M}_{\rm ph}$ beyond r_g is sufficiently large, no hydrogen and helium may be left in the nebula when Uranus and Neptune acquired large enough core masses to enter the rapid gas-gathering phase.

As we have shown in section II.D.1 above, the EUV photoevaporative mass loss rate caused by the central star varies as $\Phi^{1/2}$. If the photoionization rate $\Phi_{\rm i}$ of the primitive sun equals 10^{41} s^{-1} for ~10^7 yr, an amount of mass comparable to a minimum solar nebula could have been removed by such a process from the outer disk beyond $r_g \approx 10$ AU in this period. The rate $\Phi_{\rm i} = 10^{41}$ s^{-1} exceeds the ultraviolet output of the present Sun by two orders of magnitude, but it is compatible with the observed output of classical T Tauri stars (cTTSs) (see, e.g., Gahm et al. 1979; Bertout 1989). To explain the loss of gases from the Earth's primitive atmosphere by hydrodynamic "blow-off," other workers have postulated EUV rates $\Phi_{\rm i} \sim 10^{41}$ s^{-1} from the early sun lasting for a few hundred million years (Sekiya et al. 1980; Hunten 1985, 1993; Zahnle and Kasting 1986), so assuming this rate for 10^7 yr is conservative in comparison.

Mass accretion from the inner disk onto the stellar surface (Bertout et al. 1988), possibly aided by magnetic fields (Königl 1991), may provide

the simplest explanation for the ultraviolet excesses of cTTSs. According to the empirical evidence presented by Strom et al. (1989, 1993), the cTTS phase lasts about 10^7 yr. If the cTTSs have outer disks that do not contain much more gas than a minimum solar nebula (see, e.g., Beckwith et al. 1990; Terebey et al. 1993), then photoevaporation may well cause the giant planets that form beyond r_g to be gas-poor giants of the ilk of Uranus and Neptune.

We discussed in section II.D.1 how the early sun may have had a strong, partially ionized wind that may have absorbed EUV photons from the sun but may itself have produced an EUV and FUV diffuse field. This effect has not been studied, and may well affect the mass loss rate and to a much lesser extent, r_g. However, the basic point that significant mass loss occurs at a radius outside Saturn's orbit but inside that of Uranus remains valid.

Shu et al. (1993) speculated that the solar nebula actually formed with a mass much greater than the minimum mass. Giant planets that formed early, when the outer disk was still massive, were pushed by the viscous evolution of the disk into the protosun. Eventually the combination of viscous accretion and photoevaporation lowered the gas mass exterior to Jupiter's orbit to a value less than a few times Jupiter's mass. At this point, the gas could no longer push the giant planets into the protosun, and the remaining gases were dispersed or accreted onto the giant planets. By this way of thinking, the "minimum solar nebula" does not define the mass of Jupiter; rather the mass of Jupiter defines the conditions of the "protoplanetary" nebula. When the role of photoevaporation is added, this line of thought has the additional noteworthy implication that the resultant disk properties may also automatically produce transitional-case planets like Saturn and gas-poor planets like Uranus and Neptune.

4. Photoevaporation of Circumstellar Disks by an External Star. For low-mass stars born in clusters, a significant fraction of the UV photons incident on the protoplanetary disks may be produced by nearby massive stars and may significantly enhance the photoevaporation process. The "proplyds" (externally ionized *prot*o*pl*anetar*y* *d*isk*s*) in the Orion Nebula are the best example of this scenario and have been extensively studied (Bally et al. 1998; O'Dell 1998 and references therein). The Trapezium cluster, whose most massive member, θ^1Ori C, resides at the cluster center and produces the H II region, contains over 700 stars with a peak density of 5×10^4 pc^{-3} in the central 0.1-pc-diameter core (McCaughrean and Stauffer 1994). Within the H II region over 150 proplyds are visible as small ($r \lesssim 100$ AU) ionized envelopes surrounding low-mass stars. Churchwell et al. (1987), using radio continuum observations, first proposed that evaporating circumstellar disks produced the envelopes. More recently, the HST has imaged numerous disks as silhouettes, either against the nebula background (McCaughrean and O'Dell 1996) or against the background ionized envelope (Bally et al. 1998). The disks glow in [O I] 6300 Å emission as well (Bally et al. 1998).

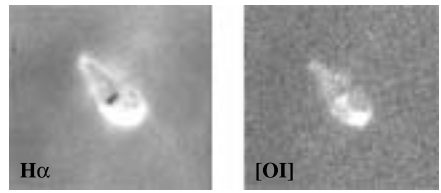

Figure 5. Hubble Space Telescope images of HST 182-413 (HST 10) in Hα (left) and [O I] 6300 Å (right). The disk appears in absorption for most optical lines except [O I]. The ionization front, seen clearly in Hα, is offset from the disk surface (Johnstone et al. 1998).

In Fig. 5 we show two narrowband images of proplyd HST 182-413 (HST 10). The head-tail appearance is characteristic of all proplyds, with the head pointing toward θ^1Ori C (although not always exactly). HST 182-413 contains a disk ($r_d \simeq 100\,\mathrm{AU}$) visible as an edge-on silhouette in all filters except [O I] and H_2 (Chen et al. 1998), where the disk emits. Surrounding the disk, yet well offset, is an envelope of ionized gas (the teardrop shape bright emission). As we shall discuss below, neutral material is removed from the disk surface at a rate higher than the incident EUV flux can keep entirely ionized, producing the offset ionization front.

In this section we discuss the photoevaporation of circumstellar disks by external stars using the Orion Nebula observations as a guide. The first assumption made in models of externally illuminated disks is that the disk radius $r_d > r_g$, so that evaporation occurs. For externally illuminated disks, this means that r_g effectively drops out of the problem. The incident EUV or FUV flux sets up a flow of constant mass flux from the disk surface for $r > r_g$. In contrast to photoevaporative flows caused by the central star, where the mass loss was dominated by the *inner* $r \sim r_g$ or r_w region close to the source, the mass loss for external illumination is dominated by the *outer* $r \sim r_d$ region, where most of the surface area lies.

Since most of the mass loss is from $r \sim r_d$, the evaporation from the disk can be approximated by the evaporation from a sphere of radius r_d. Pressure gradients in the flow will cause the streamlines to diverge rapidly beyond r_d and approximate spherical outflow. The "surface" of the disk (sphere), for the purposes of photoevaporation, can be defined as the sonic surface, where the disk flow changes from subsonic to supersonic flow. As discussed in section II.D.1, it lies at the point where the EUV or FUV flux is attenuated to the point of just heating the gas to a temperature such that the sound speed equals the escape speed. If EUV dominates at the sonic point, either dust or recombinations can attenuate the flux. If FUV dominates, then dust is the prime opacity source. Let n_0 be the gas density at the disk surface or sonic point. Then the photoevaporative mass loss from the sphere is given by $\dot{M}_{\rm ph} \simeq m_{\rm H} n_0 c_s 4\pi r_d^2$, where c_s is the sound speed in the heated (10^4 K ionized or $\sim 10^3$ K neutral) flow. Therefore, to

calculate $\dot{M}_{\rm ph}$, one need only estimate n_0. The base density n_0 is given by the condition that the EUV or FUV be (just) absorbed in the flow.

If dust dominates the EUV or FUV opacity, then the dust optical depth $\tau_{\rm UV}$ in the flow is proportional to the gas column density N_D in the flow. Because the density falls off rapidly due to spherical divergence, $N_D \simeq n_0 r_d$. For interstellar dust, $N_D \simeq 10^{21}$ cm^{-2} gives $\tau_{\rm UV} \simeq 1$. Given that N_D is fixed to give $\tau_{\rm UV} \sim$ few, it follows that $n_0 \propto r_d^{-1}$; the base density is smaller for larger disks. In the case $n_0 r_d \sim$ constant, $\dot{M}_{\rm ph}$ is quite independent of the incident UV flux (as long as it is sufficient to heat the gas so that $c_s \sim$ constant), and $\dot{M}_{\rm ph} \propto r_d$.

If recombinations dominate the EUV opacity, then the recombinations in a radial column ($\sim \frac{1}{3}\alpha_r n_0^2 r_d$, where α_r is the recombination coefficient for 10^4 K ionized gas) balance the incident EUV flux ($F_i = \Phi_i/(4\pi d^2)$, where d is the distance to the EUV source). In this case, $\dot{M}_{\rm ph}$ depends on the incident EUV flux ($\dot{M}_{\rm ph} \propto F_i^{1/2}$) and $\dot{M}_{\rm ph} \propto \Phi_i^{1/2} d^{-1} r_d^{3/2}$.

Johnstone et al. (1998) and Störzer and Hollenbach (1999) have showed that the photoevaporation rates of disks around low-mass stars illuminated by nearby massive stars may either be dominated by the EUV or the FUV photon flux from the high-mass star. In the case of EUV-dominated flow, a thin PDR region ($\Delta r \lesssim r_d$) is produced at the disk surface by the FUV flux, but the neutral gas moves subsonically through the PDR to the ionization front (IF), where the flow is ionized, heated to 10^4 K, and accelerated to supersonic speeds, $v_f \gtrsim 10$ km s^{-1}. The mass loss rate, if recombinations dominate the opacity, is given from the above

$$\dot{M}_{\rm ph}^{\rm EUV} \simeq 7 \times 10^{-9}\ {\rm M}_\odot\ {\rm yr}^{-1} \left(\frac{\Phi_i}{10^{49}\ {\rm s}^{-1}}\right)^{1/2} \left(\frac{r_d}{10\ {\rm AU}}\right)^{3/2} \left(\frac{10^{17}\ {\rm cm}}{d}\right)$$

where $\Phi_i \sim 10^{49}$ s^{-1} for an early O star as nearby neighbor.

On the other hand, in FUV-dominated flows, the FUV produces sufficient PDR pressure that a supersonic neutral flow is launched from the disk surface. The ionizing EUV flux cannot penetrate this opaque flow until its density has dropped significantly. The ionized H II flow commences in an IF at a standoff distance $r_{\rm IF} \gtrsim 2 r_d$. Moving outwards from the disk surface, the supersonic neutral wind first passes through a shock, decelerates to subsonic speeds, forms a thick subsonic layer, and then passes through a stationary IF at $r_{\rm IF}$ where the flow is heated to 10^4 K and reaccelerated to supersonic ($v_f \gtrsim 10$ km s^{-1}) speeds. The mass loss rate in this case can be approximated

$$\dot{M}_{\rm ph}^{\rm FUV} \simeq 2 \times 10^{-8}\ {\rm M}_\odot\ {\rm yr}^{-1} \left(\frac{N_D}{5 \times 10^{21}\ {\rm cm}^{-2}}\right)\left(\frac{r_d}{10\ {\rm AU}}\right)$$

where N_D ($\sim 5 \times 10^{21}$ cm^{-2} in the numerical studies of Störzer and Hollenbach 1999) is the column density from the ionization front to the sonic point (disk surface).

Given the UV flux incident on the disk and the disk size r_d, the photoevaporation model predicts $r_{\rm IF}$, with only one "free" parameter, the UV opacity of the dust grains in the flow. Approximately 10 proplyds have been observed in Orion, where both r_d and $r_{\rm IF}$ are directly measured with some accuracy (Johnstone et al. 1998). Störzer and Hollenbach (1999) used these sources to derive an average UV dust opacity in the evaporating flows and found a dust cross section per hydrogen nucleus of $\sigma_{\rm UV} \simeq 8 \times 10^{-22}$ cm^2. This value is only a factor of 2 or 3 less than diffuse interstellar values, and compatible with Orion Nebula or dense molecular cloud values (Draine and Bertoldi 1996). Therefore, consistent with the expectations of settling and coagulation of dust particles in disks (Weidenschilling 1984; Weidenschilling and Cuzzi 1993), the abundance of small ($\sim$100 Å) dust particles, which dominate the UV opacity, is relatively unchanged in the upper atmospheres of these young ($t \lesssim 10^6$ yr) disks at 10–100 AU.

Using this value for $\sigma_{\rm UV}$, Störzer and Hollenbach (1999) derive the parameter space for EUV- and FUV-dominated flows for the proplyds in Orion. FUV-dominated flows occur roughly when 10 AU $\lesssim r_d \lesssim$ 100 AU and when 0.01 pc $\lesssim d \lesssim$ 0.3 pc, where d is the distance to the dominant UV source θ^1 Ori C. For large distances or small disks, the FUV cannot heat the PDR to sufficient temperature to drive evaporative flow (i.e., $c_s < v_{\rm escape}$). For small distances or large disks, the EUV penetrates close to the disk surface and determines the mass loss.

Johnstone et al. (1998) and Störzer and Hollenbach (1999) analyzed the observational data from approximately 40 proplyds and showed that many of the flows, including HST 182-413 (Fig. 5), are likely to be FUV-dominated. Störzer and Hollenbach (1998, 1999) further showed that the FUV-dominated flow models match perfectly with the observed intensities of the optical emission near the IF as well as the neutral [O I] 6300 Å and H_2 2-μm intensities coming from the disk surface. Henney and Arthur (1998) show that a photoevaporation model fits the observed falloff in optical emission with distance from the proplyd. Johnstone et al. (1998) proposed that the observed tails of the comet-shaped ionization fronts could be caused by the diffuse UV radiation driving an FUV-dominated flow from the shadowed side of the proplyd. Figure 6 shows a numerical confirmation of this proposal from Richling and Yorke (1999). The numerical study used such a large disk ($r_d \sim 300$ AU) that the front side is EUV-dominated. Nevertheless, on the back side an FUV-dominated flow with an IF shaped like the observed tails is seen in the simulation. All these results give added confidence in the validity of the FUV-dominated photoevaporation models.

Assuming that $\sigma_{\rm UV}$ is approximately the same for all the observed proplyds, the theoretical models are able to predict the disk sizes from the observed sizes of the ionization fronts. Johnstone et al. (1998) derived the disk radii for approximately 30 proplyds in which $r_{\rm IF}$ was measured but where the disk could not be seen. The disk radii ranged from 10 to 100 AU.

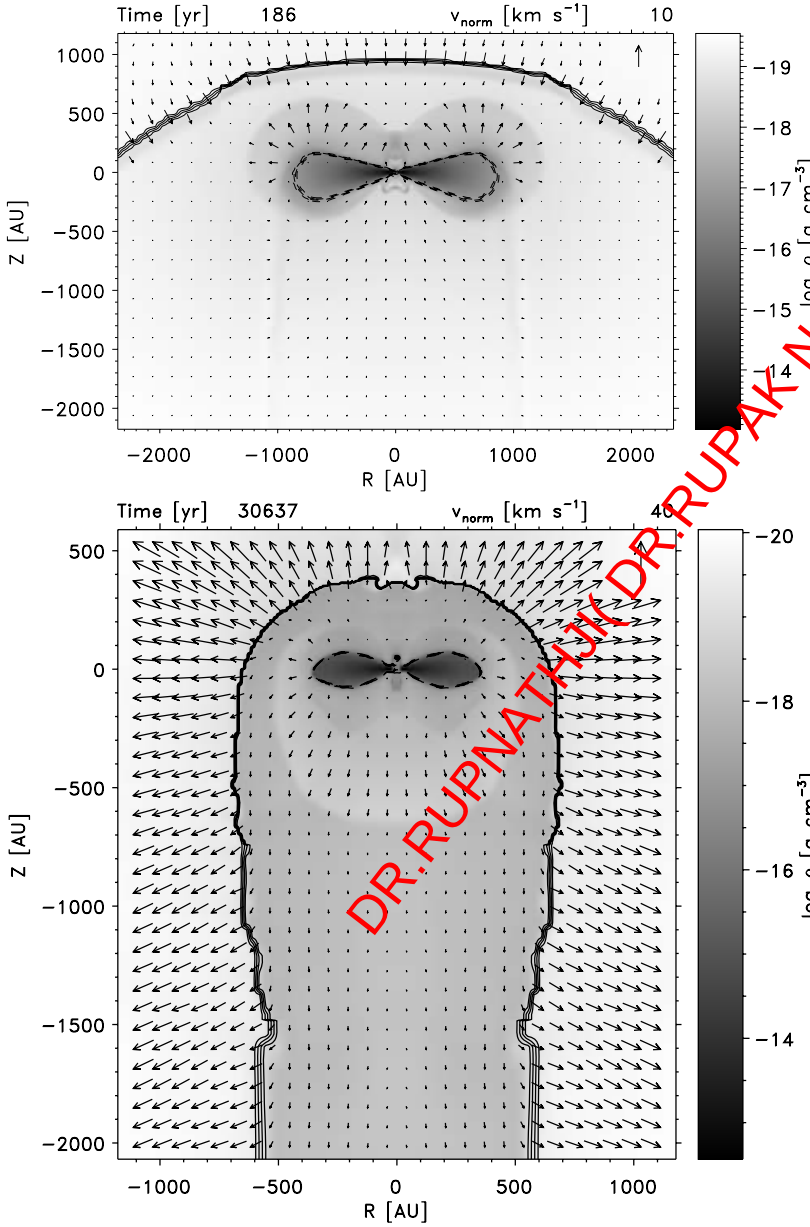

Figure 6. Numerical simulations of the photoionization and photoevaporation of circumstellar disks by an external EUV and FUV source (Richling and Yorke 1998*b*). The top frame depicts an early stage after the sudden turn-on of the source located above the disk, with fluxes $f_{\rm EUV} = 6.3 \times 10^{12}$ cm^{-2} s^{-1} and $f_{\rm FUV} = 1.6 \times 10^{13}$ cm^{-2} s^{-1}. The appearance at this time of a second simulation with a higher FUV flux $f_{\rm FUV} = 1.3 \times 10^{14}$ cm^{-2} s^{-1} is nearly identical. The bottom frame shows the quasi-steady-state result of this simulation. Note the significant reduction of disk size due to removal of the loosely bound outer disk material. The FUV-dominated flow on the back side creates a cometlike tail.

If the proplyds are in circular orbits around the UV source θ^1 Ori C, so that d is constant in time, Johnstone et al. (1998) and Störzer and Hollenbach (1999) showed how the current disk mass M_d could be estimated from the current $\dot{M}_{\rm ph}$ and the disk illumination time t_i. Assuming that the surface density in the disk scales as $\Sigma \propto r^{-\beta}$, where $1 < \beta < 2$, most of the mass in the disk is at $r \sim r_d$, the disk evaporates from outside in, and the timescale for evaporation $t_{\rm evap}$ increases as the disk shrinks. (Note that $t_{\rm evap} = M_d/\dot{M}_{\rm ph}$ is not the timescale for complete dispersal, but only for the mass and radius to decrease by factors of order 2). If the disks initially are large enough that they have shrunk significantly after time t_i, $M_d \simeq \dot{M}_{\rm ph} t_i$. Millimeter-wave observations (Lada 1998) detect two disks with $M_d \sim 0.01$ M$_\odot$ and limit several others to smaller masses. Observed and theoretical estimates (Johnstone et al. 1998; Störzer and Hollenbach 1999) of $\dot{M}_{\rm ph} \gtrsim 10^{-7}$ M$_\odot$ yr^{-1} then limit $t_i < 10^5$ yr. In the case of circular orbits, it appears that θ^1 Ori C must be less than 10^5 years old, surprisingly small compared to the $\sim 10^6$-yr age estimated for the low-mass stars in the cluster (Hillenbrand 1997).

On the other hand, the proplyds are likely to be on much more eccentric orbits around θ^1 Ori C. (Note that the cluster potential is dominated by the distributed mass for $d \gtrsim 0.05$ pc, so the orbits are not Keplerian in any case.) Störzer and Hollenbach (1999) considered the opposite extreme of radial orbits and showed that, in this case, the disks may shrink and lose mass as they approach θ^1 Ori C. However, inside a critical distance $d_{\rm cr}$, their dynamical time is shorter than $t_{\rm evap}$, so they move quickly through the central region "frozen" in mass and size. For disks that have experienced significant shrinkage and which lie inside of $d_{\rm cr}$ (as most of the ~40 well-studied proplyds do), the current mass of the disk is approximately $M_d \simeq \dot{M}_{\rm ph}(d_{\rm cr}/v)$, where $\dot{M}_{\rm ph}$ is evaluated at $d_{\rm cr}$ and where $d_{\rm cr}/v$ is the crossing time t_c for a proplyd moving at v through the central region. Hillenbrand and Hartmann (1998) estimate $v \simeq 2.3$ km s^{-1}, or $t_c \simeq 10^5$ yr. Störzer and Hollenbach (1999) derive theoretically that $d_{\rm cr} \simeq 0.2$ pc and that $\dot{M}_{\rm ph}$ at $d_{\rm cr}$ is roughly fitted by the analytic approximation to numerical models $\dot{M}_{\rm ph} \simeq 10^{-7}(r_d/100\ {\rm AU})^{1-1.5}$ M$_\odot$ yr^{-1}. Therefore, the disk masses for shrunken proplyds passing near ($d < d_{\rm cr}$) θ^1Ori C are given by $M_d \simeq 10^{-2}(r_d/100\ {\rm AU})^{1-1.5}$ M$_\odot$; the disk masses are roughly proportional to their sizes. Since most of the 40 well-studied proplyds have $r_d \lesssim 100$ AU, the models predict $M_d \lesssim 10^{-2}$ M$_\odot$, in agreement with observation. In this case of radial orbits, there is no need for θ^1Ori C to be exceptionally young. The Trapezium cluster extends to $d \sim 2$ pc, has a half-mass radius of $d \sim 0.5$ pc, and a typical crossing time across the whole cluster of $\sim 10^6$ yr (Hillenbrand and Hartmann 1998). If θ^1Ori C is $\sim 10^6$ years old and the entire cluster is on radial orbits, then each of the ~1000 proplyds in the cluster has passed close to θ^1Ori C roughly one time and has photoevaporated to $r_d \sim$ 10–100 AU. We presently observe mostly the nearby bright objects inside of $d_{\rm cr}$. Those foreground proplyds

that have not passed through the central regions and have stayed outside the H II region ($d \gtrsim 0.6$–1 pc), perhaps because their orbits are more circular, remain large ($r_d \sim 100$–500 AU) and are observed as silhouettes (McCaughrean and O'Dell 1996). In the case of the Trapezium cluster, one O star has significantly affected the disk evolution of perhaps hundreds of low-mass stars like the Sun through the process of photoevaporation.

Although it appears that most stars in the Galaxy are formed in clusters (Lada et al. 1991; Lada 1992; Bonnell and Kroupa 1998) and that these clusters have sizes 0.1–1 pc, it is not clear how many stars form in a typical cluster. If that number is greater than about 100, then it is very likely that an O or B star will form among its members, and that photoevaporation by an an external star will affect the fate of most planet-forming disks in the Galaxy. In Fig. 1 we have also plotted the photoevaporation timescale t_E(evap) as a function of r for disks around low-mass stars in clusters like the Trapezium cluster.

III. CONCLUSIONS

Figure 1 shows the timescales for various gas (and small dust) dispersal mechanisms in planet-forming disks as a function of the position r in the disk. The stellar encounter lifetime t_{SE} is plotted for Trapezium-like conditions ($n_\star = 10^4$ pc^{-3} and $v = 1$ km s^{-1}) and clearly is only important in the outer regions, $r \gtrsim 100$ AU, of planet-forming disks in dense clusters. The viscous timescale t_ν is plotted for two representative values of α and are seen to be dominant in the inner, $r < 10$ AU, parts of disks. The wind timescales, t_{ws} and t'_{ws}, are plotted assuming a minimum-mass ($M_d \simeq 0.01$ M$_\odot$) disk with $\beta = 3/2$ and with $\epsilon(\sin\theta)^2 = 10^{-4}$. Wind mass loss rates of $\dot{M}_w = 10^{-8}$ M$_\odot$ yr^{-1} are assumed for t_{ws}; in the t'_{ws} case, we have assumed that the wind mass loss rate declines with time as $\dot{M}_w = 10^{-6}(10^5 \text{ yr}/t)$ M$_\odot$ yr^{-1} for $t < 10^7$ yr. The winds are assumed to be spherically symmetric. Although there is considerable uncertainty in $\epsilon(\sin\theta)^2$, it appears that stellar wind stripping is not particularly effective, in contrast to the commonly held view of the dispersal of the solar nebula. The photoevaporation timescale caused by the central star, t_c(evap), is plotted assuming $\Phi_i = 10^{41}$ s^{-1}, the "strong wind" case, and a minimum-mass nebula with $\beta = 3/2$. The photoevaporation timescale caused by an external star, t_E(evap), is plotted for Trapezium conditions, assuming radial orbits, a cluster of size 1 pc, and a minimum-mass nebula with $\beta = 3/2$. The photoevaporation timescales become very long at $r < 10$ AU because the stellar gravity holds the disk material and prevents evaporation. Photoevaporation is generally dominant for $r > 10$ AU. Photoevaporation acting together with viscous spreading of material will remove the entire disk in timescales of order 10^7 years for the nominal parameters assumed in Fig. 1.

The rapid cutoff between Saturn and Uranus in the hydrogen and helium gas content of the giant planets may be explained by the photoevaporation of the outer, $r > 10$ AU, solar nebula early in its history before Uranus and Neptune could accumulate the gas. Shu et al. (1993) proposed that the early sun provided the UV photons. However, it is also quite possible that the solar nebula could have spent its early life in a stellar cluster, where a nearby O or B star may have photoevaporated the outer nebula in timescales $t \lesssim 10^7$ years.

Acknowledgments This work was conducted at the authors' three affiliated institutes and has been supported in part through the NASA Astrophysics Theory Program, which supports a joint Center for Star Formation Studies at NASA/Ames Research Center, UC Berkeley, and UC Santa Cruz; in part through NASA sponsorship at Jet Propulsion Laboratory, California Institute of Technology, within the "Origins" Program; and in part through funding by the Natural Sciences and Engineering Research Council of Canada.

REFERENCES

Adams, F. C., Emerson, J. P., and Fuller, G. A. 1990. Submillimeter photometry and disk masses of T Tauri disk systems. *Astrophys. J.* 357:606–620.

Balbus, S. A., and Hawley, J. F. 1991. A powerful local shear instability in weakly magnetized disks. I: Linear analysis. II: Nonlinear evolution. *Astrophys. J.* 376:214–233.

Bally, J., and Scoville, N. Z. 1982. Structure and evolution of molecular clouds near H II regions. II: The disk constrained H II region, S106. *Astrophys. J.* 255:497–509.

Bally, J., Sutherland, R. S., Devine, D., and Johnstone, D. 1998. Externally illuminated young stellar environments in the Orion Nebula: Hubble Space Telescope planetary camera and ultraviolet observations. *Astron J.* 116:293–321.

Beckwith, S. V. W., Sargent, A. I., Chini, R. S., and Guesten, R. 1990. A survey for circumstellar disks around young stellar objects. *Astron J.* 99:924–945.

Bertout, C. 1989. T Tauri stars: Wild as dust. *Ann. Rev. Astron. Astrophys.* 27:351–395.

Bertout, C., Basri, G., and Bouvier, J. 1988. Accretion disks around T Tauri stars. *Astrophys. J.* 330:350–373.

Bodenheimer, P., and Pollack, J. B. 1986. Calculations of the accretion and evolution of giant planets: The effects of solid cores. *Icarus* 67:391–408.

Bonnell, I., and Kroupa, P. 1998. Dynamical interactions in dense stellar clusters. In *The Orion Complex Revisited,* Astronomical Society of the Pacific Conf. Series, ed. M. J. McCaughrean and A. Burkert, in press.

Burrows, C. J., Stapelfeldt, K. R., Watson, A. M., Krist, J. E., Ballester, G. E., Clarke, J. T., Crisp, D., Gallagher, J. S., Griffiths, R. E., Hester, J. J., Hoessel, J. G., Holtzman, J. A., Mould, J. R., Scowen, P. A., Trauger, J. T., and

Westphal, J. A. 1996. Hubble Space Telescope observations of the disk and jet of HH 30. *Astrophys. J.* 473:437–451.
Cameron, A. G. W. 1973. Accumulation processes in the primitive solar nebula. *Icarus* 18:407–450.
Cameron, A. G. W. 1978. Physics of the primitive solar nebula and of giant gaseous protoplanets. In *Protostars and Planets,* ed. T. Gehrels and M. S. Matthews (Tucson: University of Arizona Press), pp. 453–487.
Cameron, A. G. W. 1995. The first ten million years in the solar nebula. *Meteoritics* 30:133–161.
Canto, J., and Raga, A. 1991. Mixing layers in stellar outflows. *Astrophys. J.* 372:646–658.
Chen, H., Bally, J., O'Dell, C. R. McCaughrean, M. J., Thompson, R. L., Rieke, M., Schneider, G., and Young, E. T. 1998. 2.12 micron molecular hydrogen emission from circumstellar disks embedded in the Orion Nebula. *Astrophys. J. Lett.* 492:L173–L176.
Churchwell, E., Felli, M., Wood, D. O. S., and Massi, M. 1987. Solar system sized condensations in the Orion Nebula. *Astrophys. J.* 321:516–529.
Clarke, C. J., and Pringle, J. E. 1993. Accretion disc response to a stellar fly-by. *Mon. Not. Roy. Astron. Soc.* 261:190–202.
Draine, B. T., and Bertoldi, F. 1996. Structure of stationary photodissociation fronts. *Astrophys. J.* 468:269–289.
Elmegreen, B. G. 1978. On the interaction between a strong stellar wind and a surrounding disk nebula. *Moon Plan.* 19:261–267.
Elmegreen, B. G. 1979. On the disruption of a protoplanetary disk nebula by a T Tauri like solar wind. *Astron. Astrophys.* 80:77–78.
Gahm, G. F., Fredga, K., Liseau, R., and Dravins, D. 1979. The far-UV spectrum of the T Tauri star RU Lupi. *Astron. Astrophys.* 73:L4–L6.
Goldreich, P., and Tremaine, S. 1979. The excitation of density waves at the Lindblad and corotation resonances by an external potential. *Astrophys. J.* 233:857–871.
Goldreich, P., and Tremaine S. 1980. Disk–satellite interactions. *Astrophys. J.* 241:425–441.
Greenberg, R., Hartmann, W. K., Chapman, C. R., and Wacker, J. F. 1978. Planetesimals to planets: Numerical simulation of collisional evolution. *Icarus* 35:1–26.
Greenberg, R., Weidenschilling, S., Chapman, C. R., and Davis, D. R. 1984. From icy planetesimals to outer planets and comets. *Icarus* 59:87–113.
Hall, S. M., Clarke, C. J., and Pringle, J. E. 1996. Energetics of star-disc encounters in the nonlinear regime. *Mon. Not. Roy. Astron. Soc.* 278:303–320.
Hartmann, L., Calvet, N., Gullbring, E., and D'Alessio, P. 1998. Accretion and the evolution of T Tauri disks. *Astrophys. J.* 495:385–400.
Hayashi, C., Nakazawa, K., and Nakagawa, Y. 1985. Formation of the solar system. In *Protostars and Planets II,* ed. D. C. Black and M. S. Matthews (Tucson: University of Arizona Press), pp. 1100–1153.
Heller, C. H. 1995. Encounters with protostellar disks. II: Disruption and binary formation. *Astrophys. J.* 455:252–259.
Henney, W. J., and Arthur, S. J. 1998. Modeling the brightness profiles of the Orion proplyds. *Astron J.* 116:322–335.
Hillenbrand, L. 1997. On the stellar population and star-forming history of the Orion Nebula cluster. *Astron J.* 113:1733–1768.
Hillenbrand, L., and Hartmann, L. 1998. A preliminary study of the Orion Nebula Cluster structure and dynamics. *Astrophys. J.* 492:540–553.
Hollenbach, D., and Tielens, A. G. G. M. 1997. Dense photodissociation regions (PDRs). *Ann. Rev. Astron. Astrophys.* 35:179–216.

Hollenbach, D., Johnstone, D., and Shu, F. 1993. Photoevaporation of disks around massive stars and ultracompact H II regions. In *Massive Stars: Their Lives in the Interstellar Medium,* ed. J. P. Cassinelli and E. B. Churchwell, Astronomical Society of the Pacific Conf. Series 35, pp. 26–34.

Hollenbach, D., Johnstone, D., Lizano, S., and Shu, F. 1994. Photoevaporation of disks around massive stars and application to ultracompact H II regions. *Astrophys. J.* 428:654–669.

Horedt, G. P. 1978. Blowoff of the protoplanetary cloud by a T Tauri-like solar wind. *Astron. Astrophys.* 64:173–178.

Horedt, G. P. 1980. Mass loss from planetary protoatmospheres and from the protoplanetary nebula. *Astron. Astrophys.* 92:267–272.

Horedt, G. P. 1982. Mass loss from the protoplanetary nebula. *Astron. Astrophys.* 110:209–214.

Hourigan, K., and Ward, W. R. 1984. Radial migration of preplanetary material: Implications for the accretion time scale problem. *Icarus* 60:29–39.

Hunten, D. M. 1985. Blowoff of an atmosphere and possible application to Io. *Geophys. Res. Lett.* 12:271–273.

Hunten, D. M. 1993. Atmospheric evolution of the terrestrial planets. *Science* 259:915–920.

Johnstone, D., Hollenbach, D., and Bally, J. 1998. Photoevaporation of disks and clumps by nearby massive stars: Application to disk destruction in the Orion Nebula. *Astrophys. J.* 499:758–776.

Kepner, J., Hartigan, P., Yang, C., and Strom, S. 1993. Hubble Space Telescope images of the subarcsecond jet in DG Tauri. *Astrophys. J. Lett.* 415:L119–L121.

Kessel, O., Richling, S., Yorke, H. W. 1998. Photoevaporation of protostellar disks. III: The appearance of photoevaporating disks around young intermediate stars. *Astron. Astrophys.* 337:832–846.

Koerner, D. W., Sargent, A. I., and Beckwith, S. V. W. 1993. A rotating gaseous disk around the T Tauri star GM Aurigae? *Icarus* 106:2–10.

Königl, A. 1991. Disk accretion onto magnetic T Tauri stars. *Astrophys. J. Lett.* 370:39–43.

Königl, A. 1995. Disk-driven hydromagnetic winds in young stellar objects. *Rev. Mex. Astron. Astrofis. Ser. Conf.* 1:275–283.

Lada, E. A. 1992. Global star formation in the L1630 molecular cloud. *Astrophys. J. Lett.* 393:L25–L28.

Lada, E. A. 1998. Observations of star formation: The role of embedded clusters. In *Origins,* ed. C. E. Woodward, J. M. Shull, and H. A. Thronson (San Francisco: ASP Publishing), pp. 198–202.

Lada, E. A., Evans, N. J., De Poy, D. L., and Gatley, I. 1991. A 2.2-micron survey in the L1630 molecular cloud. *Astrophys. J.* 371:171–182.

Larwood, J. D. 1997. The tidal disruption of protoplanetary accretion discs. *Mon. Not. Roy. Astron. Soc.* 290:490–504.

Laughlin, G., and Bodenheimer P. 1994. Nonaxisymmetric evolution in protostellar disks. *Astrophys. J.* 436:335–354.

Lin, D. N. C., and Papaloizou, J. 1979. Tidal torques on accretion discs in binary systems with extreme mass ratios. *Mon. Not. Roy. Astron. Soc.* 186:799–812.

Lin, D. N. C., and Papaloizou, J. 1985. On the dynamical origin of the solar system. *Protostars and Planets II,* ed. D. C. Black and M. S. Matthews (Tucson: University of Arizona Press), 981–1071.

Lin, D. N. C., and Papaloizou, J. 1986*a*. On the tidal interaction between protoplanets and the primordial solar nebula. II: Self-consistent nonlinear interaction. *Astrophys. J.* 307:395–409.

Lin, D. N. C., and Papaloizou, J. 1986*b*. On the tidal interaction between protoplanets and the protoplanetary disk. III: Orbital migration of protoplanets. *Astrophys. J.* 309:846–857.
Lin, D. N. C., Bodenheimer P., and Richardson, D. C. 1996. Orbital migration of the planetary companion of 51 Pegasi to its present location. *Nature* 380:606–607.
Lissauer, J. J. 1987. Timescales for planetary accretion and the structure of the protoplanetary disk. *Icarus* 69:249–265.
Lissauer, J. J. 1993. Planet formation. *Ann. Rev. Astron. Astrophys.* 31:129–174.
McCaughrean, M. J., and O'Dell, C. R. 1996. Direct imaging of circumstellar disks in the Orion Nebula. *Astron J.* 111:1977–1986.
McCaughrean, M. J., and Stauffer, J. R. 1994. High-resolution near-infrared imaging of the Trapezium: A stellar census. *Astron J.* 106:1382–1397.
Mizuno, H. 1980. Formation of the giant planets. *Prog. Theor. Phys.* 64:544–557.
Nakagawa, Y., Hayashi, C., and Nakazawa, K. 1983. Accumulation of planetesimals in the solar nebula. *Icarus* 54:361–376.
O'Dell, C. R. 1998. Observational properties of the Orion Nebula proplyds. *Astron. J.* 115:263–273.
Ohtsuki, K., and Nakagawa, Y. 1988. Accumulation process of planetesimals to the planets. *Prog. Theor. Phys. Suppl.* 96:239–255.
Ouyed, R., and Pudritz, R. 1997*a*. Numerical simulations of astrophysical disks. I: Stationary models. *Astrophys. J.* 482:712–732.
Ouyed, R., and Pudritz, R. 1997*b*. Numerical simulations of astrophysical disks. II: Episodic outflows. *Astrophys. J.* 484:794–809.
Papaloizou, J., and Lin, D. N. C. 1984. On the tidal interaction between protoplanets and the primordial solar nebula. I: Linear calculation of the role of angular momentum exchange. *Astrophys. J.* 285:818–834.
Pechernikova, G. V., and Vitjazev, A. V. 1981. Thermal dissipation of gas from the protoplanetary cloud. *Adv. Space Res.* 1:55–60.
Pollack, J. B., Hubickyj, O., Bodenheimer P., Lissauer, J. J., Podolak, M., and Greenzweig, Y. 1996. Formation of the giant planets by concurrent accretion of solids and gas. *Icarus* 124:62–85.
Pringle, J. E., and Rees, M. J. 1972. Accretion disc models for compact X-ray sources. *Astron. Astrophys.* 21:1–9.
Richling, S., and Yorke, H. W. 1997. Photoevaporation of protostellar disks. II: The importance of UV dust properties and ionizing flux. *Astron. Astrophys.* 327:317–324.
Richling, S., and Yorke, H. W. 1998. Photoevaporation of protostellar disks. IV. Externally illuminated disks. *Astron. Astrophys.* 340:508–520.
Richling, S., and Yorke, H. W. 1999. Photoevaporation of protostellar disks. IV: Circumstellar disks under the influence of both EUV and FUV. *Astrophys. J.,* submitted.
Safronov, V. S. 1969. *Evolution of the protoplanetary cloud and formation of Earth and the Planets* (Moscow: Nauka).
Sekiya, M., Nakazawa, K., and Hayashi, C. 1980. Dissipation of the rare gases contained in the primordial Earth's atmosphere. *Earth Plan. Sci. Lett.* 50:197–201.
Shakura, N. I., and Sunyaev, R. A. 1973. Black holes in binary systems: Observational appearance. *Astron. Astrophys.* 24:337–355.
Shu, F. H., Lizano, S., Ruden, S. P., and Najita, J. 1988. Mass loss from rapidly rotating magnetic protostars. *Astrophys. J.* 328:L19–L23.
Shu, F. H., Johnstone, D., and Hollenbach, D. 1993. Photoevaporation of the solar nebula and the formation of the giant planets. *Icarus* 106:92–101.

Stapelfeldt, K. R., Burrows, C. J., Krist, J., Watson, A. M., Trauger, J. T., Ballester, G. E., Casertano, S., Clarke, J. T., Crisp, D., Evans, R. W., Gallagher, J. S., Griffiths, R. E., Hester, J. J., Hoessel, J. G., Holtzman, J., Mould, J. R., Scowen, D. A., and Westphal, J. A. 1994. WFPC2 observations of the HH 30 disk and jet. *Bull. Amer. Astron. Soc.* 185:4802.

Störzer, H., and Hollenbach, D. 1998. On the [O I] lambda 6300-line emission from the photoevaporating circumstellar disks in the Orion Nebula. *Astrophys. J. Lett.* 502:L71–L74.

Störzer, H., and Hollenbach, D. 1999. PDR models of photoevaporating circumstellar disks and application to the proplyds in Orion. *Astrophys. J.*515:669–684.

Strom, K. M., Strom, S. E., Edwards, S., Cabrit, S., and Skrutskie, M. F. 1989. Circumstellar material associated with solar-type pre-main-sequence stars: A possible constraint on the timescale for planet building. *Astron J.* 97:1451–1470.

Strom, S. E., 1995. Initial frequency, lifetime and evolution of YSO disks. *Rev. Mex. Astron. Astrofis.* 1:317–328.

Strom, S. E., Edwards, S., and Skrutskie, M. F. 1993. Evolutionary time scales for circumstellar disks associated with intermediate- and solar-type stars. In *Protostars and Planets III,* ed. E. H. Levy and J. I. Lunine (Tucson: University of Arizona Press), pp. 837–866.

Terebey, S., Shu, F. H., and Cassen, P. 1984. The collapse of the cores of slowly rotating isothermal clouds. *Astrophys. J.* 286:529–551.

Terebey, S., Chandler, C. J., and André, P. 1993. The contribution of disks and envelopes to the millimeter continuum emission from very young low-mass stars. *Astrophys. J.* 414:759–772.

van Buren, D. 1985. The initial mass function and global rates of mass, momentum, and energy input to the interstellar medium via stellar winds. *Astrophys. J.* 294:567–577.

Ward, W. R. 1986. Density waves in the solar nebula: Differential Lindblad torque. *Icarus* 67:164–180.

Weidenschilling, S. J. 1984. Evolution of grains in a turbulent solar nebula. *Icarus* 60:553–567.

Weidenschilling, S. J., and Cuzzi, J. N. 1993. Formation of planetesimals in the solar nebula. In *Protostars and Planets III,* pp. 1031–1060.

Wetherill, G. W. 1980. Formation of the terrestrial planets. *Ann. Rev. Astron. Astrophys.* 18:77–113.

Wetherill, G. W., and Stewart, G. R. 1986. The early stages of planetesimal accumulation. *Lun. Plan. Sci.* 17:939.

Wood, D. O. S., and Churchwell, E. 1989. The morphologies and physical properties of ultracompact H II regions. *Astrophys. J. Suppl.* 69:831–895.

Yorke, H. W., and Welz, A. 1993. In *Star Formation, Galaxies and the Interstellar Medium,* ed. J. Franco, F. Ferrini, and G. Tenorio-Tagle (Cambridge University Press), pp. 239–244.

Yorke, H. W., and Welz, A. 1994. In *Numerical Simulations in Astrophysics.* ed. J. Franco, S. Lizano, L. Aguilar, and E. Daltabuit (Cambridge University Press), pp. 318–326.

Yorke, H. W., and Welz, A. 1996. Photoevaporation of protostellar disks. I: The evolution of disks around early B stars. *Astron. Astrophys.* 315:555–564.

Yorke, H. W., Bodenheimer P., and Laughlin, G. 1995. The formation of protostellar disks. II: Disks around intermediate-mass stars. *Astrophys. J.* 443:199–208.

Zahnle, K .J., and Kasting, J. F. 1986. Mass fractionation during transonic escape and implications for loss of water from Mars and Venus. *Icarus* 68:462–480.